

Frequency of Collapsing Precipitation Cores within the Eyewalls of U.S. Landfalling Hurricanes (1994-2007)

Keith G. Blackwell*
Department of Earth Sciences
University of South Alabama, Mobile, Alabama

Jeffrey Medlin
National Weather Service Forecast Office
Mobile Alabama

1. INTRODUCTION

Holmes et al., 2006 identified massive collapsing cores (CCs) of heavy precipitation within the “open” eyewalls of Hurricanes Ivan and Katrina at landfall on the northern Gulf Coast. Holmes et al. stated that their very preliminary investigation indicated that these

types of features were more common in “open eyewall” storms as opposed to “closed eyewall” storms. The current study investigates some aspects of CC climatology in all hurricanes which have come within 60 nautical miles of coastal WSR-88D Doppler radars in the U.S. (and one storm near Puerto Rico) between 1994 and 2007 (Table 1).

Year	Storm Name	Saf-Sim Category	Landfall Location	Wind (kts)	Pressure (hPa)	Intensity Change	Eye Character	CC Activity (>50 dBZ)
1995	Erin	1	FL-East	75	984	S	Open	Moderate
1995	Erin	2	FL-NW	85	973	I	Closed	Moderate
1995	Opal	3	FL-NW	100	942	W	Open	Moderate [#]
1996	Bertha	2	NC	90	960	I	Open	Low
1996	Fran	3	NC	100	954	S	Open	Moderate [#]
1997	Danny	1	LA	65	989	I	Open	Low
1997	Danny	1	AL	70	984	S	Open	Prolific
1998	Bonnie	2	NC	95	964	S	Open	Low to None
1998	Earl	1	FL-NW	70	987	S	Open	Low to None
1998	Georges	3	PR	100	968	S	Closed	Moderate
1998	Georges	2	FL-SW	90	981	I	Open	Low
1998	Georges	2	MS	90	964	W	Closed	Low
1999	Bret	3	TX-S	100	951	W	Closed	Prolific
1999	Floyd	2	NC	90	956	W	Open	Moderate
1999	Irene	1	FL-S	70	987	S	Open	Low
2002	Lili	1	LA	80	963	W	Open	Moderate
2003	Claudette	1	TX	80	979	I	Closed	Moderate
2003	Erika	1	MX-NE	65	986	I	Open	Prolific
2003	Isabel	2	NC	90	957	W	Closed	None
2004	Charley	4	FL-SW	130	941	I	Closed	Prolific
2004	Charley	1	SC	70	992	W	Open	Moderate to Low
2004	Francis	2	FL-E	90	960	I	Closed	None
2004	Gaston	1	SC	65	985	I	Open	Moderate
2004	Ivan	3	AL	105	946	W	Open	Prolific
2004	Jeanne	3	FL-E	105	950	S	Closed	Low
2005	Cindy	1	LA	65	991	I	Closed	Low
2005	Dennis	3	FL-NW	105	946	W	Closed	Prolific
2005	Katrina	1	FL-SE	70	984	I	Open	Prolific
2005	Katrina	3	LA/MS	110	920	W	Open	Moderate
2005	Ophelia	1	NC	75	979	S	Closed	Low
2005	Rita	3	LA-TX	100	937	W	Open	Prolific
2005	Wilma	3	FL-S	105	950	S	Closed	Low to None
2007	Humberto	1	TX-NE	80	985	S	Open	Prolific

[#] Activity dramatically increased inland.

Table 1. All hurricanes which have come within 60 nautical miles of WSR-88D radars in the southeast U.S. (including Georges near Puerto Rico) from 1994 and 2007. (Intensity change: S-steady, I-intensifying, W-weakening)

*Corresponding Author: Keith G. Blackwell, Department of Earth Sciences, LSCB 136, University of South Alabama, Mobile, AL 36688. E-mail: kblackwell@usouthal.edu. Phone: 251-460-6302.

2. METHODOLOGY

Doppler radar Level II archive data was acquired from the National Climatic Data Center for each of the storms listed in Table 1. Some storms experienced multiple landfalls; each landfall was treated as a separate event. Radars were selectively chosen which would provide the best coverage of each storm's inner core generally within 60 nm of the coastline. This digital Level II data was displayed and analyzed with Gibson Ridge Software's GRLevel2 Analyst Edition radar software. For this study, only extremely heavy convective areas displaying ≥ 50 dBZ reflectivity factors were analyzed.

Base reflectivity patterns were scrutinized for possible collapsing core activity. When heavy convection was observed, 3-dimensional cross sections were used to further investigate the feature. Base velocity patterns were also examined in the vicinity of the convection.

For suspected collapsing cores, information was collected, such as the:

- Location of CC relative to storm center
- percentage of the eye enclosed by immediately adjacent base reflectivities ≥ 20 dBZ and ≥ 35 dBZ.
- approximate height specifications
- approximate duration of CC event.

Only the hurricane eyewalls were examined for CC activity. For storms with multiple eyewalls, only the inner eyewalls were examined in this study in order to maintain comparison continuity.

3. RESULTS

Of the 33 landfall events depicted in Table 1, only 9 storms (27%) exhibited prolific collapsing core activity (Figure 1). In order to be categorized as a prolific CC producer, vigorous collapsing cores must be observed nearly continuously in the eyewall of the storm over a period of several hours during the landfall event.

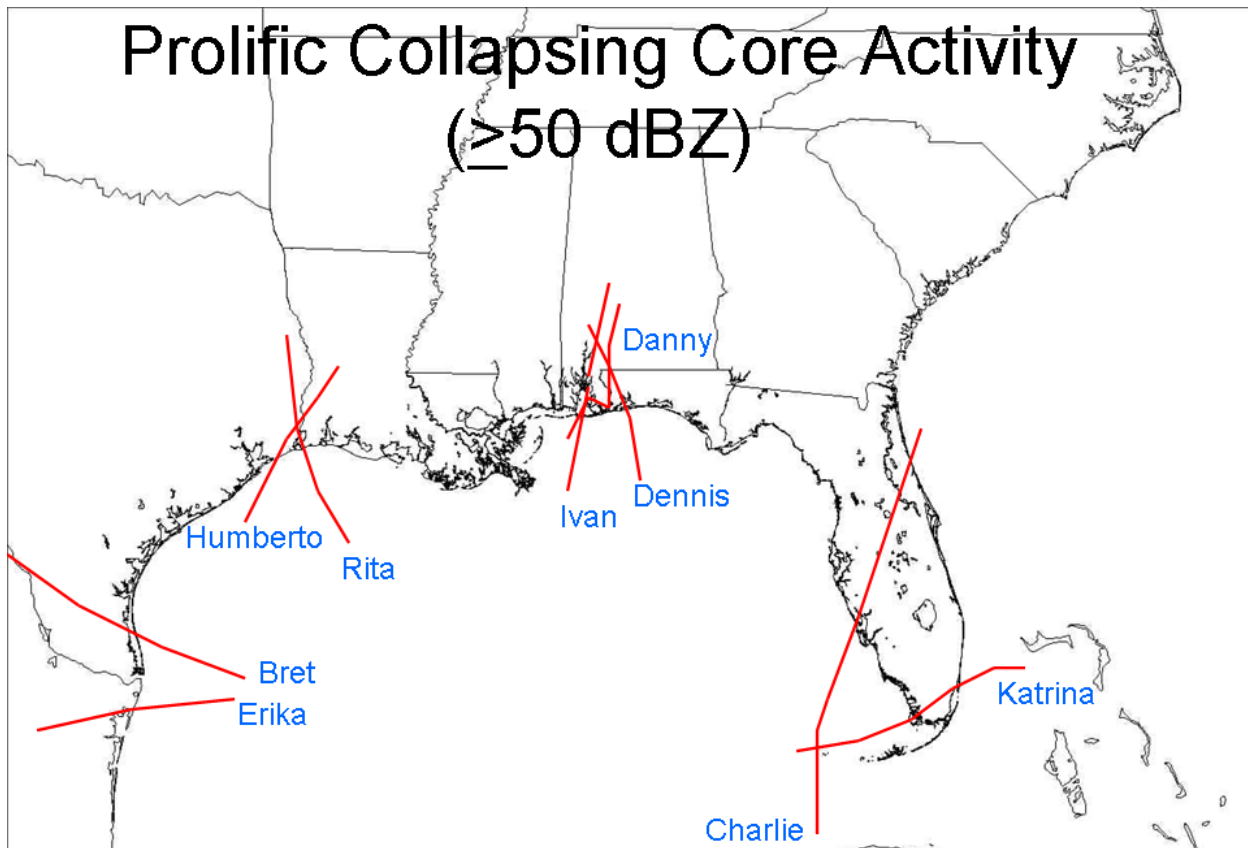


Figure 1. U.S. Hurricanes (1994-2007) which exhibited prolific collapsing precipitation core activity at landfall.

Of these 9 storms, Hurricanes Danny (Alabama landfall), Bret and Humberto were three of the most prolific CC producers.

Hurricanes designated as moderate CC producers are shown in Figure 2; eleven storms (33%) met this categorization. Often in these situations the CC activity was 1) not as vigorous as the prolific producers, or 2) occurred distinctly before or after the actual landfall, but was not particularly notable near the coast. For instance, Hurricanes Opal, Fran, and Lili produced nearly all of their CC activity over

inland areas with very little CC activity along the coast or immediately prior to landfall. However once inland, these storms produced large and sustained events over a large area (note: Level II archive data during Lili's landfall contained large temporal data gaps from nearby radars at KLCH and KPOE; KLIX indicated significant inland CC activity with Lili, but the remote distance of the radar precluded detailed analysis).

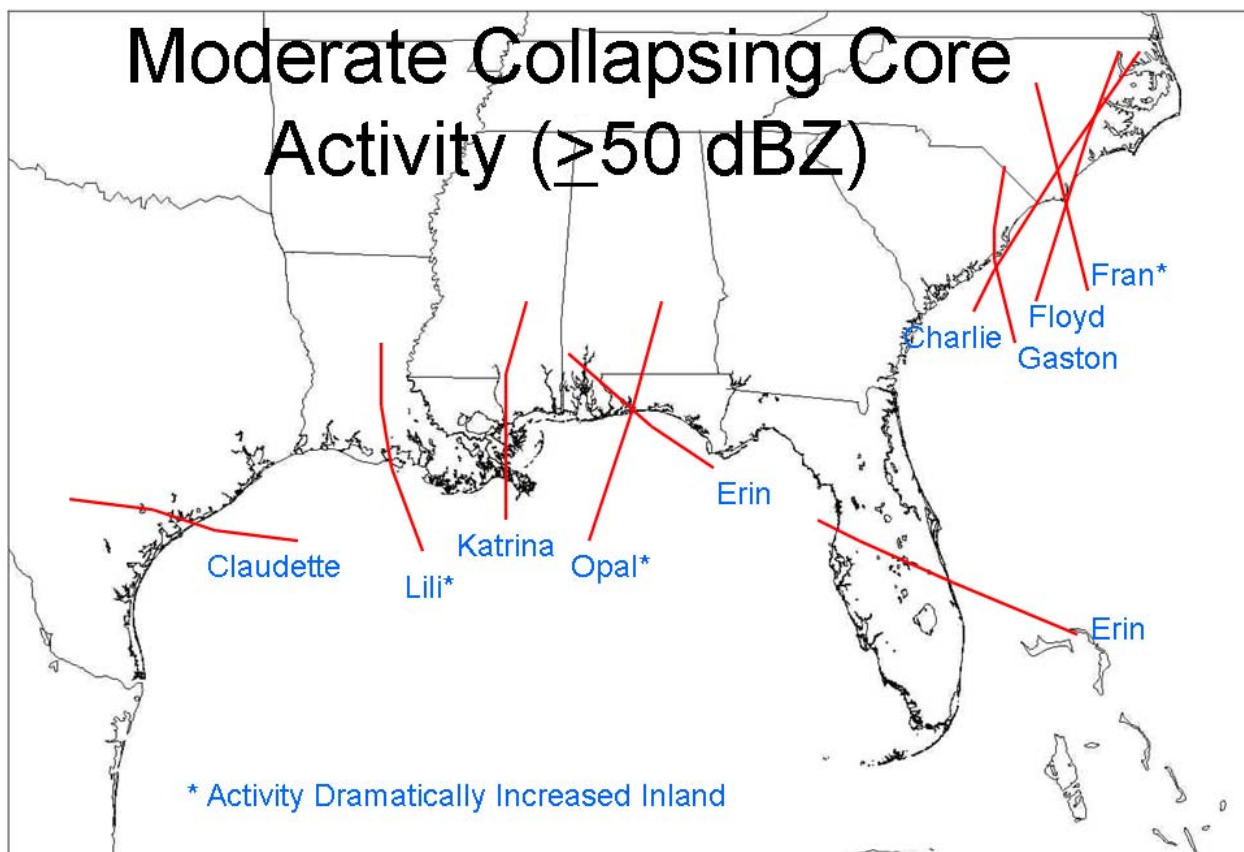


Figure 2. As in Figure 1, except for storms with moderate collapsing core activity.

Some storms produced only sporadic and weak CC activity during their landfall events while others produced absolutely no events at all (Figure 3). Storms which contained virtually no

CC activity include Bonnie, Earl, Georges (Florida Keys and Mississippi), Isabel, Frances, and Wilma. Often, these storms were virtually absent of reflectivities ≥ 50 dBZ.

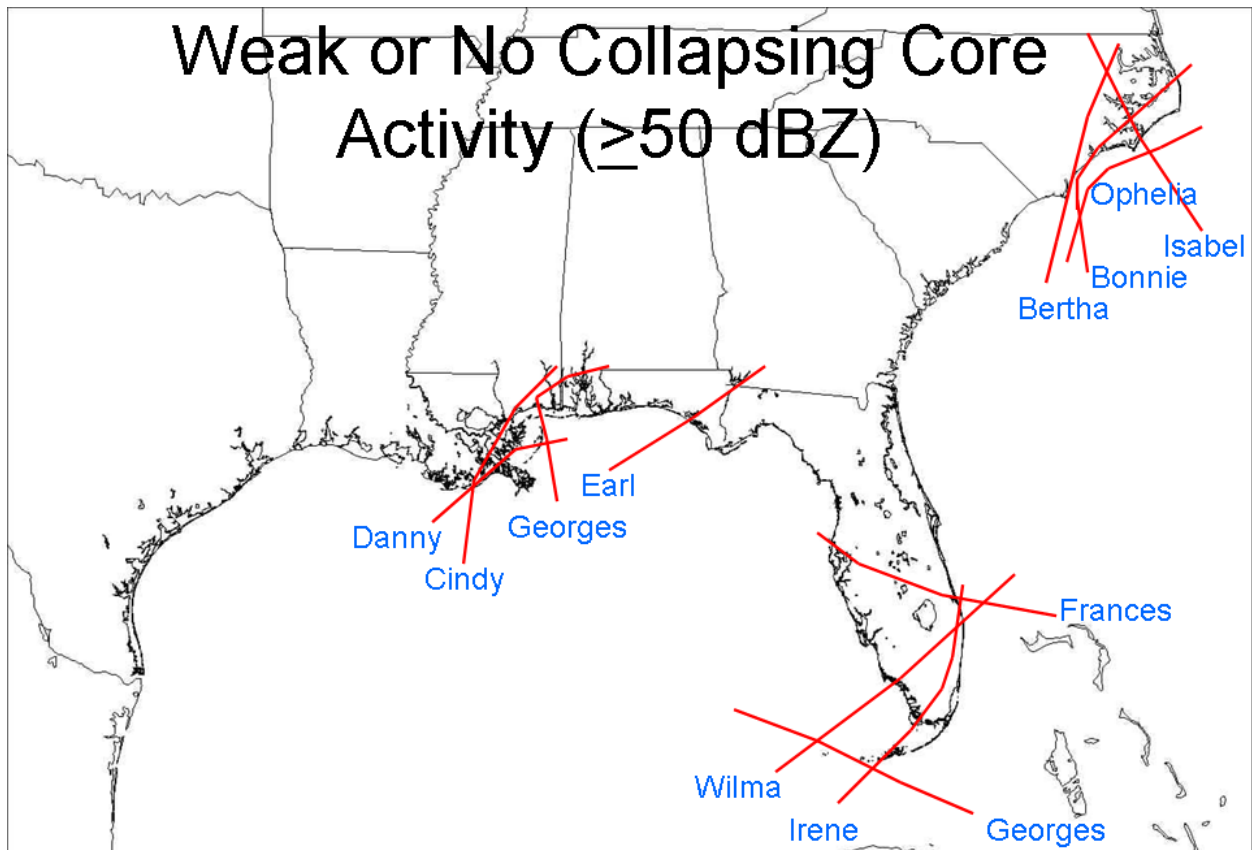


Figure 3. As in Figure 1, except for storms with little to no collapsing core activity.

Several classic CC events are depicted in Figures 4 through 11. Often, storms change character during the landfall event, or exhibit very different CC behavior between landfalls (for storms with multiple landfalls). Such is the case with Danny with minimal activity over SE Louisiana and the open Gulf, but once the storm became nearly stationary in Mobile Bay continuous and large CCs occurred in the western eyewall. Blackwell (2000) and Medlin et al., (2007) describe the character and phenomenal rainfall which occurred in this storm. Medlin et al. place Danny as one of the two greatest tropical cyclone-related precipitation events on record in the U.S.

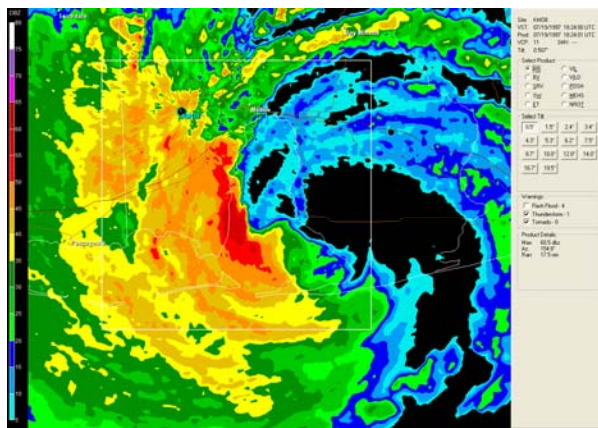
Figure 4 indicates one such CC in Danny. Figure 4a shows extremely heavy convection on the west side of Danny's center with an "inflow notch" penetrating into the convection from the northeast. This inflow notch and much of the heaviest convection is occurring within the radius of maximum wind (RMW) (see Figure 4b). Figures 4c and 4d depict a massive

overhang of ≥ 50 dBZ reflectivity extending upwind and above the inflow notch. Directly above this weak echo region associated with the inflow notch is >55 dBZ reflectivity up to an altitude of over 5,000 m ($\sim 16,000$ feet). Base reflectivities >60 dBZ are depicted 22 km (12 nm) downwind (i.e. to the south southwest) at 460 m (1180 feet) elevation. The entire elevated region of ≥ 50 dBZ "overhangs" the precipitation-free low-level jet for up to 30 km (16 nm) "upstream" of the location of similar base reflectivity values near the surface.

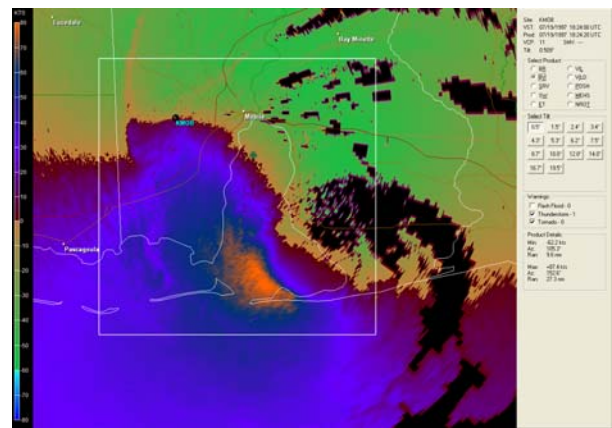
Figure 12 in Blackwell (2000) indicate an elevated jet on the dry east side of Danny. A low-level wind maximum is then found within the heavily convective west side of the storm at about 500 m altitude. Given the features shown in Figure 4 (below), this elevated jet likely extends into Danny's inflow notch within the RMW and beneath the overhanging precipitation. From there, the jet likely descends to a much lower altitude and dramatically accelerates. Very significant

downward momentum transfer within the RMW is likely occurring within Danny's nearly continuous collapsing cores of heavy precipitation over Mobile Bay; this downward momentum transfer likely continues to very low levels. Very significant surface wind gusts appear likely within and/or downwind of these

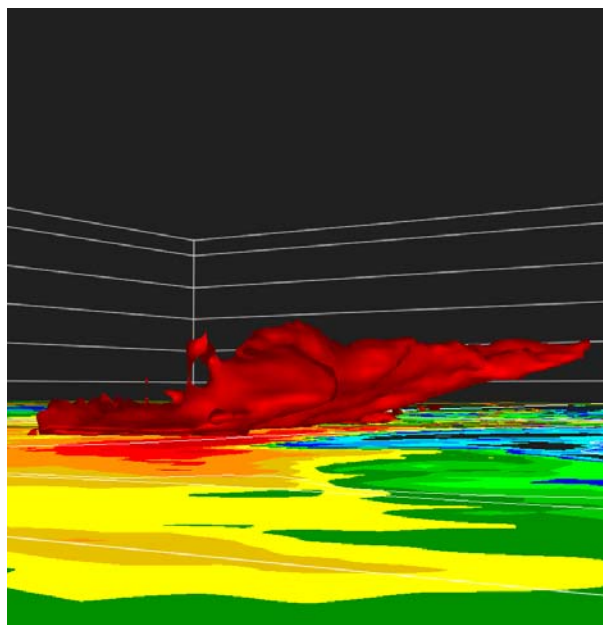
high base reflectivity values within the storm's eyewall. Indeed the maximum wind gust measured at DPIA1 on the east end of Dauphin Island during Danny likely occurred near a smaller CC event a few hours earlier.



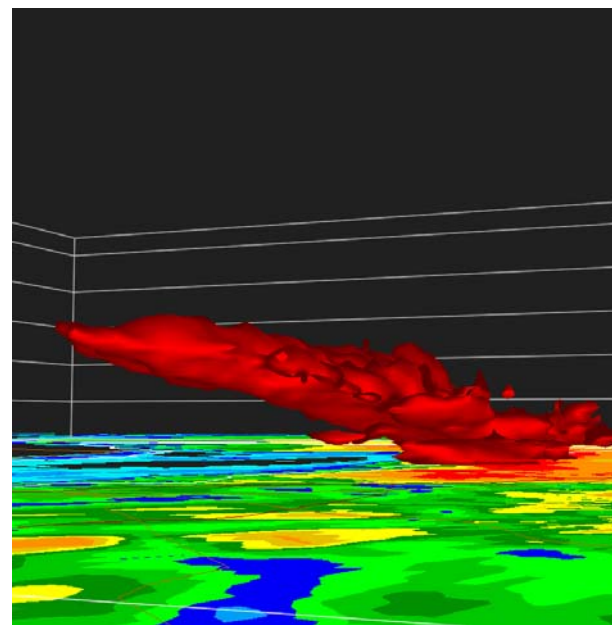
a.



b.



c.

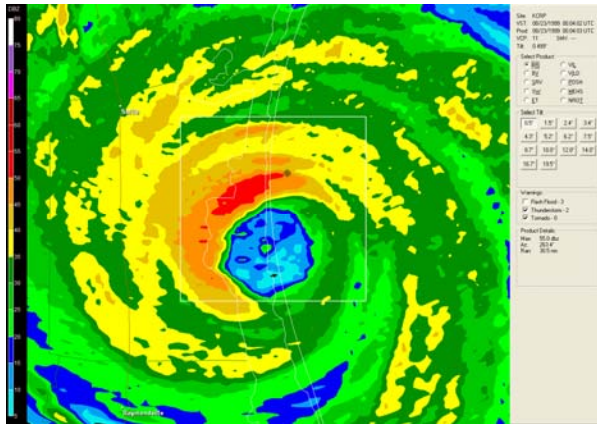


d.

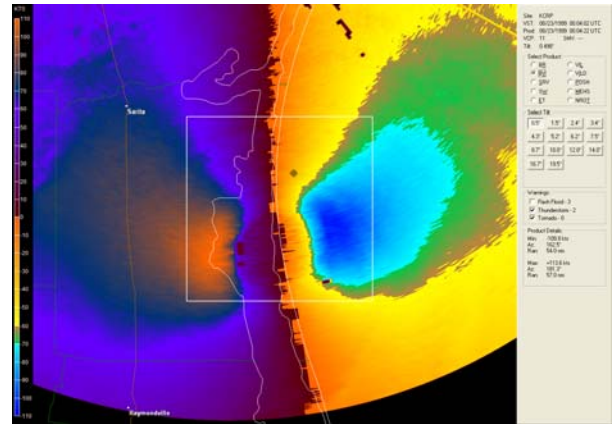
Figure 4. Collapsing cores in Hurricane Danny while situated in Mobile Bay AL at 1824 UTC, 19 July 1997 as depicted by KMOB WSR-88D Level II data. **a.** Base reflectivity. **b.** Base velocity (maximum outbound (orange)/inbound (green) velocities: 87 kt / 54 kt, respectively). Reflectivity 3-D vertical cross sections through Danny's eyewall **c.** looking northwest and **d.** looking southeast. Red shading in **a.**, **c.**, and **d.** represent reflectivities ≥ 50 dBZ. The vertical axis in **c.**, and **d.** is depicted in 10,000 foot increments [white horizontal lines]).

A similar reflectivity pattern is depicted in Hurricane Bret (Figure 5), Hurricane Charley (Figure 6), Hurricane Ivan (Figure 7), Hurricane Katrina (Figure 8), Hurricane Rita (Figure 9), and Hurricane Humberto (Figures 10 and 11). Each of these storms depict a region of very enhanced base reflectivity in the eyewall, coincident with the storm's RMW which tilts "upwind" with height and "overhangs" strong

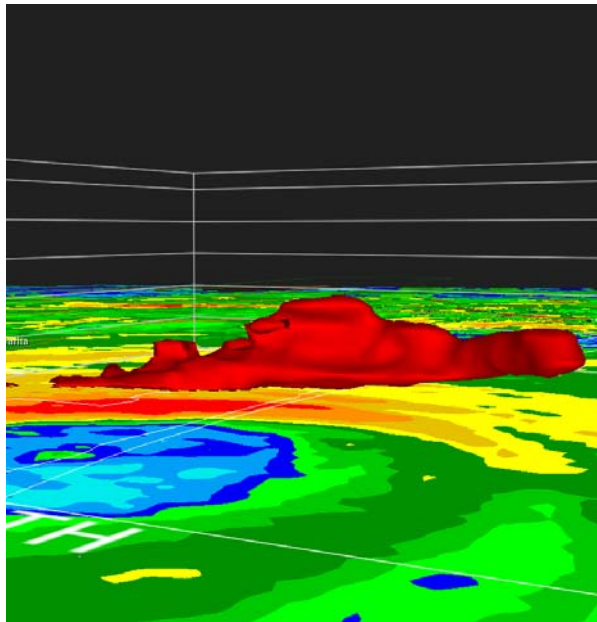
winds within the storm's RMW. It is likely that very significant downward momentum transfer is occurring within low-level wind maxima embedded within the accompanying high base reflectivity regions of these feature, likely contributing to an enhancement of the wind velocity deep into the boundary layer and much enhanced near-surface wind gusts there.



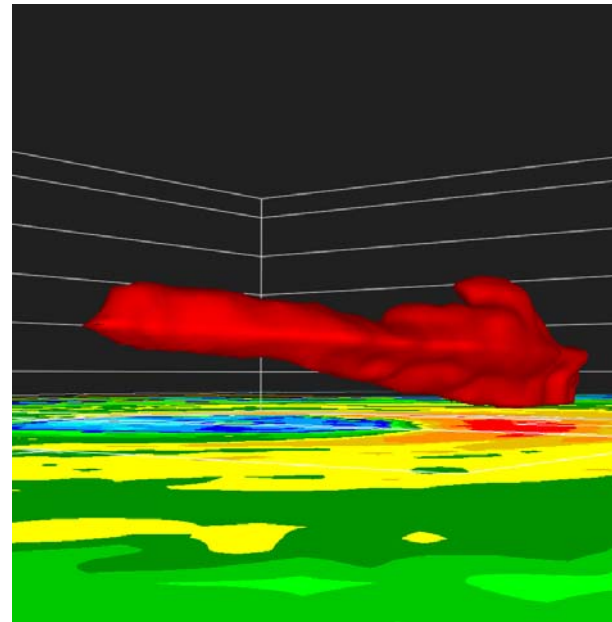
a.



b.

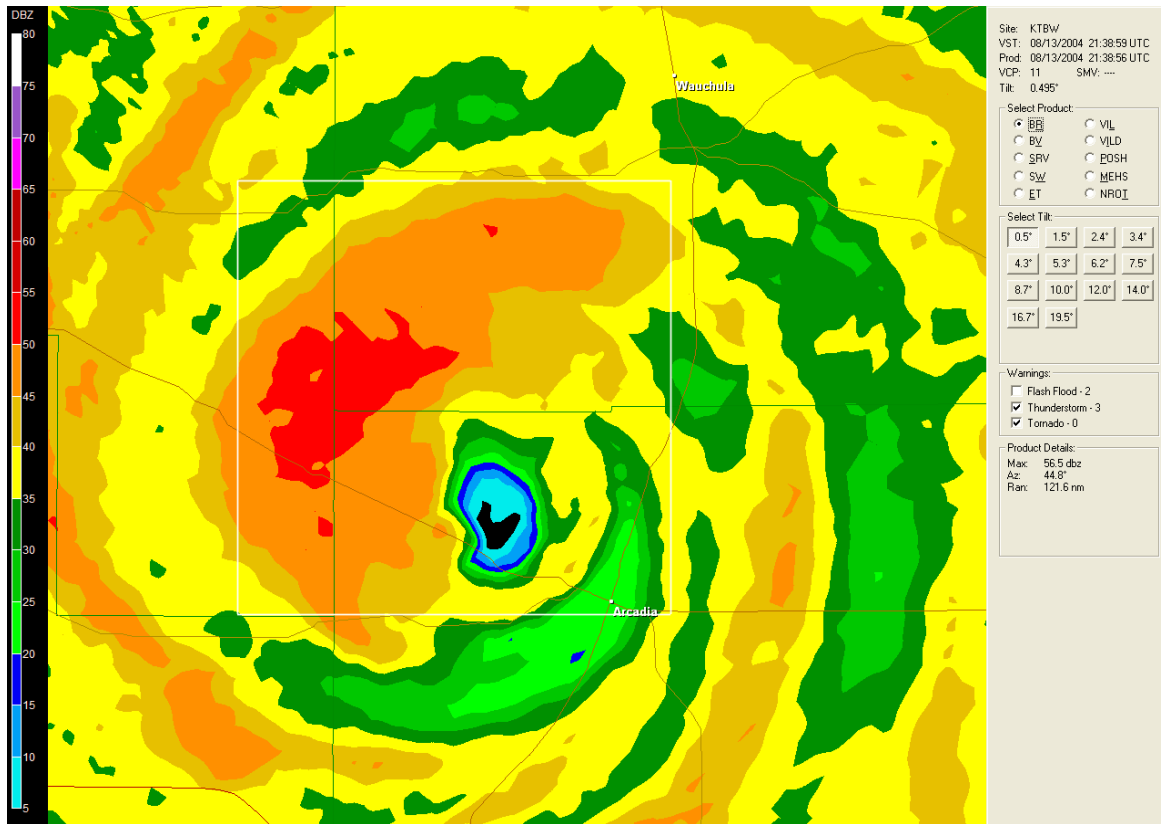


c.

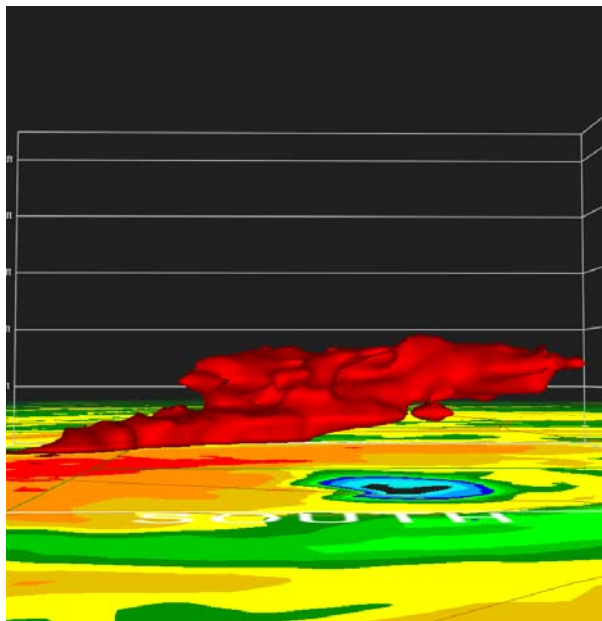


d.

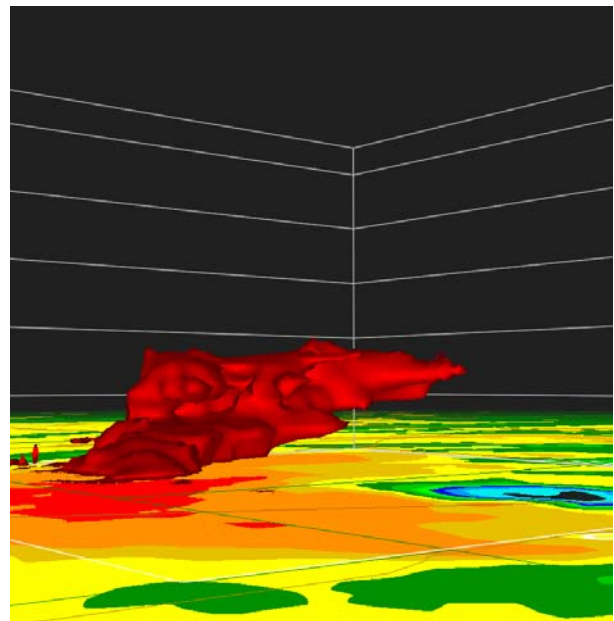
Figure 5. Collapsing cores in Hurricane Bret while making landfall near Padre Island TX at 0004 UTC, 23 August 1999 as depicted by KCRP WSR-88D Level II data. **a.** Base reflectivity. **b.** Base velocity (maximum outbound (orange)/inbound (blue) velocities: 114 kt / 108 kt respectively). Reflectivity 3-D vertical cross sections through Bret's eyewall: **c.** looking northwest and **d.** looking southwest. Red shading in **a.**, **c.**, and **d.** represent reflectivities ≥ 50 dBZ. The vertical axis in **c.**, and **d.** is depicted in 10,000 foot increments [white horizontal lines].



a.

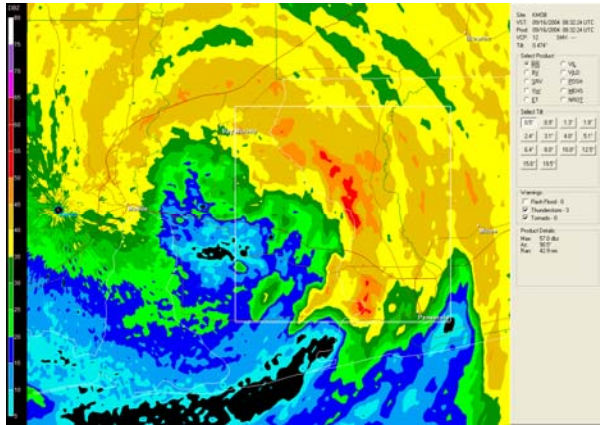


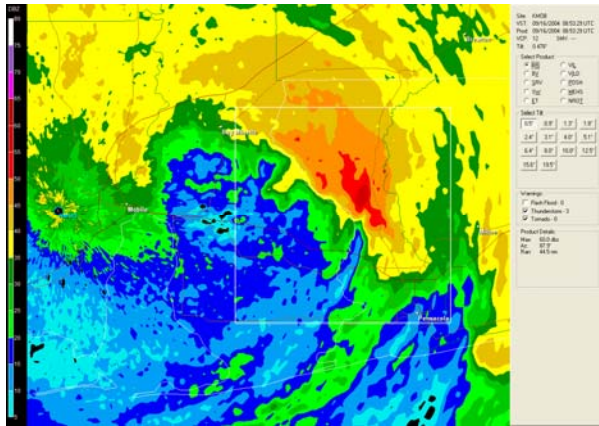
b.



c.

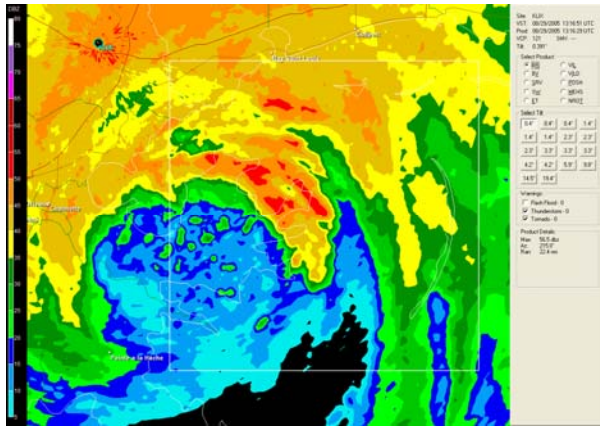
Figure 6. Collapsing cores in Hurricane Charley while inland over southwest Florida near Arcadia at 2138 UTC, 13 August 2004 as depicted by KTBW WSR-88D Level II data. **a.** Base reflectivity. Reflectivity cross sections through Charley's eyewall: **b.** looking north and **c.** looking northeast. Red shading in **a.**, **b.**, and **c.** represents reflectivities ≥ 50 dBZ. The vertical axis in **c.**, and **d.** is depicted in 10,000 foot increments [white horizontal lines]).



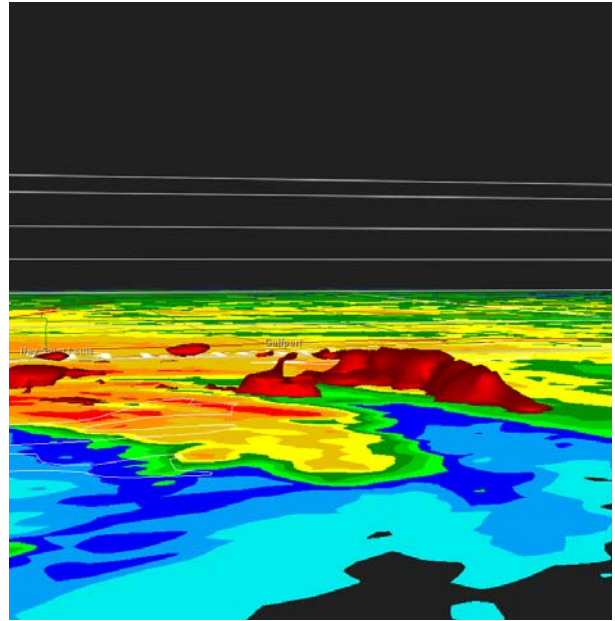


g.

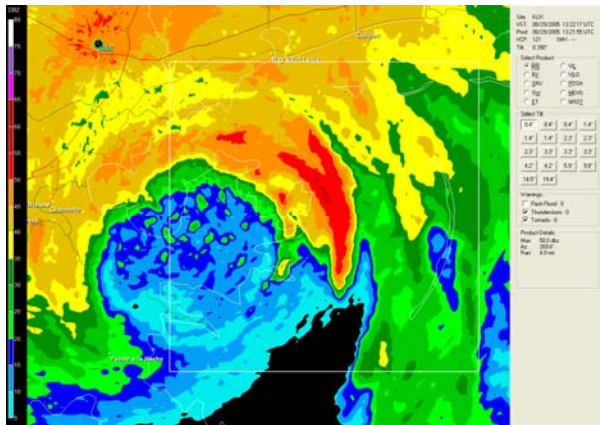
Figure 7. Sequential images of a collapsing core in Hurricane Ivan's eastern eyewall over the Alabama/Florida line to the northwest of Pensacola FL from the KMOB WSR-88D on 16 September 2004. Base reflectivity (**a.**) and corresponding reflectivity 3-D cross section (**b.**) at 0832 UTC (looking northeast). The remaining images are the same as **a.**, except in approximately 4 minute intervals at **c.** 0837 UTC, **d.** 0841 UTC, **e.** 0845 UTC, **f.** 0849 UTC, and **g.** 0853 UTC. Red shading in the images represents reflectivities ≥ 50 dBZ; The vertical axis in **b.** is depicted in 10,000 foot increments [white horizontal lines].



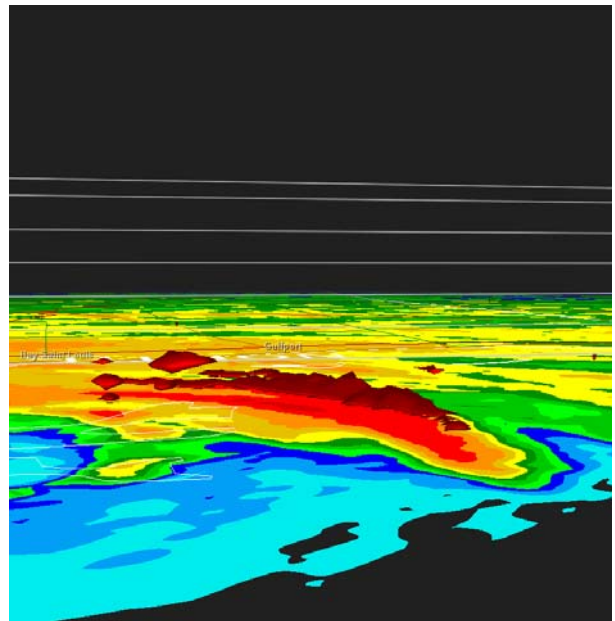
a.



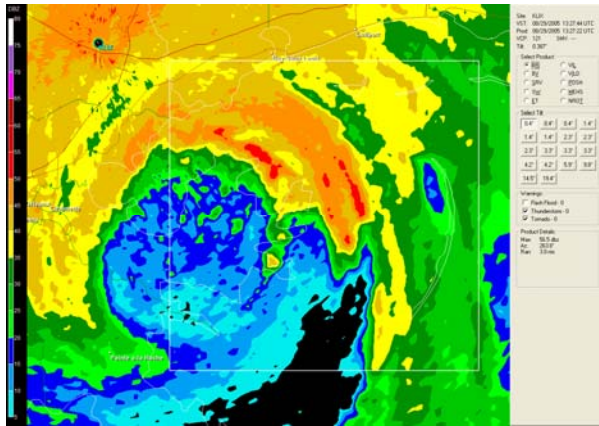
b.



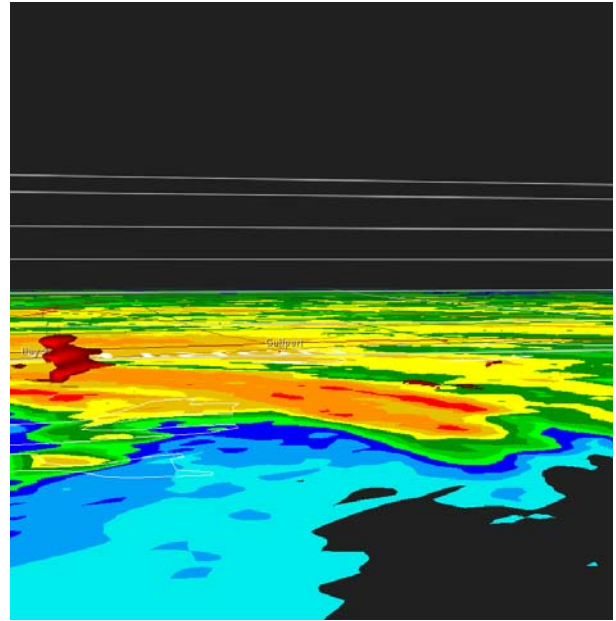
c.



d.

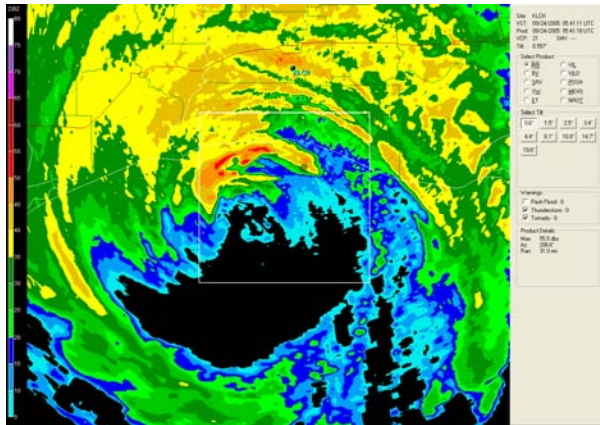


e.

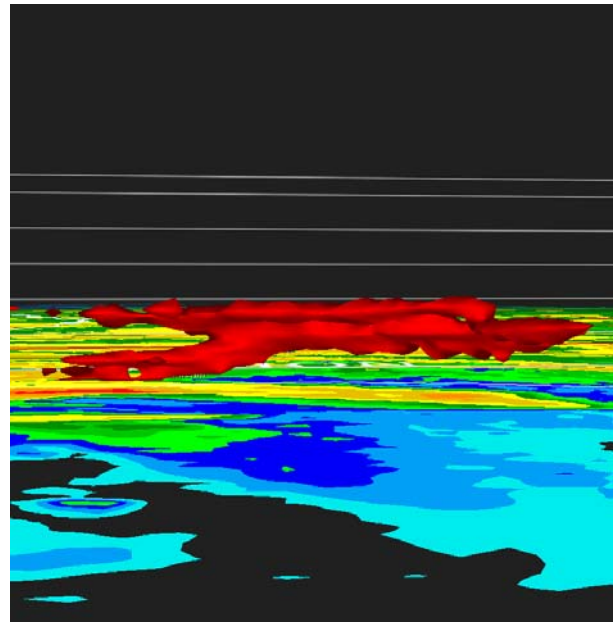


f.

Figure 8. Sequential images of a collapsing core in Hurricane Katrina's eastern inner eyewall to the south of the Mississippi coast over the Chandeleur Sound and extreme eastern St. Bernard Parish, LA from the KLIX WSR-88D on 29 August 2005. Base reflectivity (**a.**) and corresponding reflectivity 3-D cross section (**b.**) at 1316 UTC (cross section looking northeast). The remaining images are the same as **a.** and **b.** except sequentially in approximate 5 minute intervals at 1322 UTC (**c.** and **d.**), and **f.** 1327 UTC (**e.** and **f.**). Red shading in the images represents reflectivities ≥ 50 dBZ; The vertical axes in **b.**, **d.** and **f.** are depicted in 10,000 foot increments [white horizontal lines]). Note the sudden massive collapse of ≥ 50 dBZ reflectivities in Katrina's eastern eyewall in the image sequence depicted.

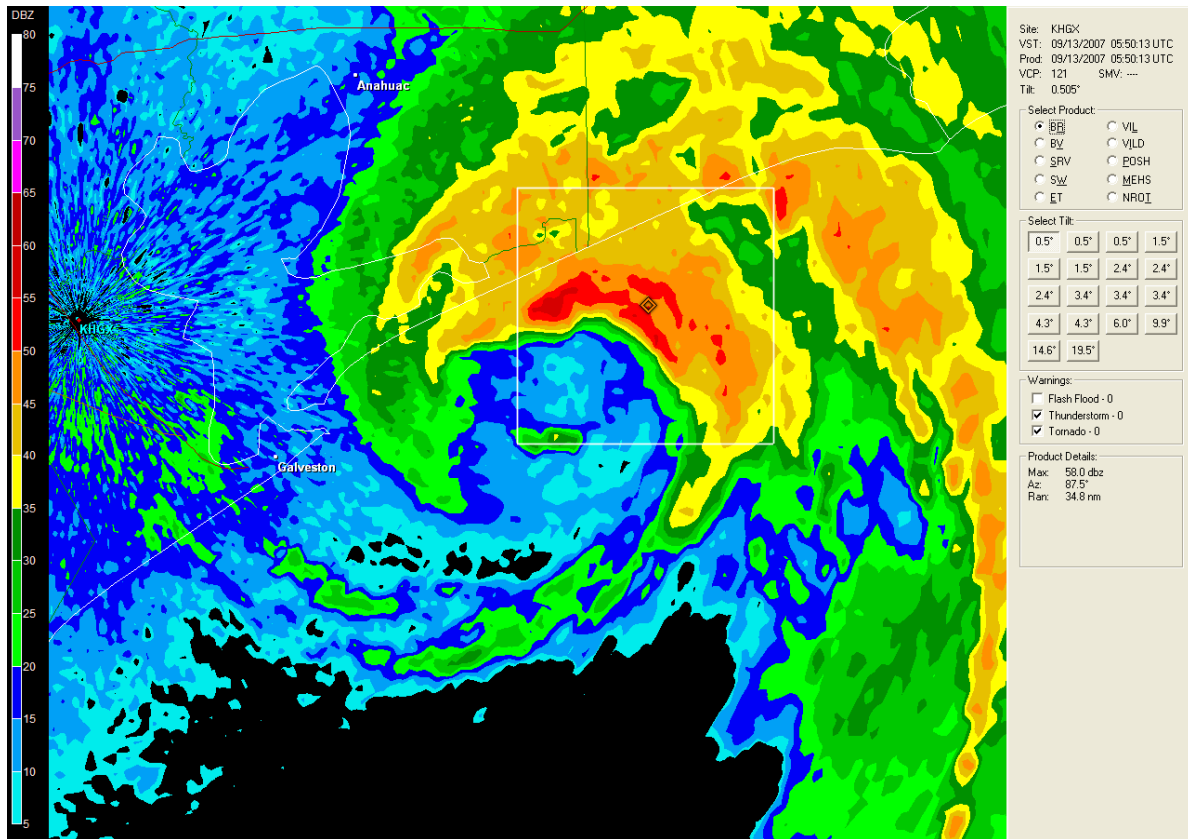


a.

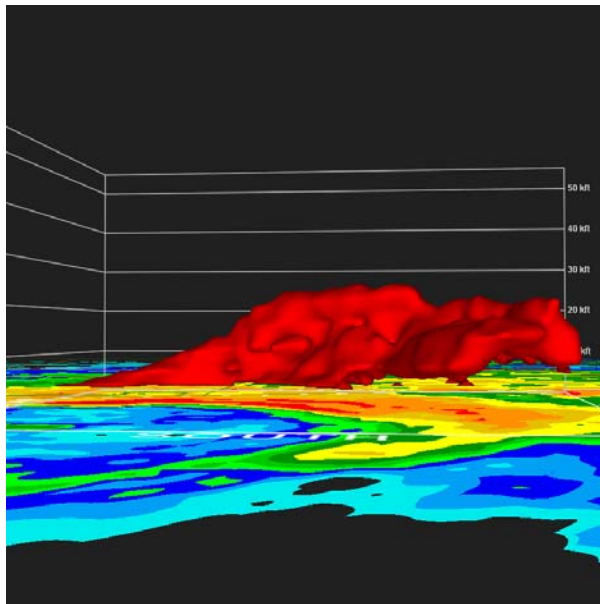


b.

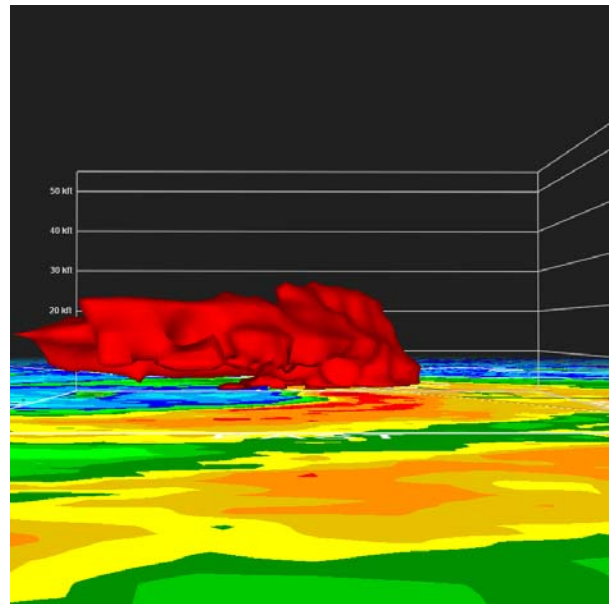
Figure 9. Base reflectivity (a.) and corresponding reflectivity 3-D cross section (b.) of a collapsing core in Hurricane Rita's northern eyewall just offshore of Cameron LA from the KLCH WSR-88D at 1316 UTC, 24 September 2005. Red shading in the images represents reflectivities ≥ 50 dBZ; The vertical axis in b. is depicted in 10,000 foot increments [white horizontal lines]).



a.



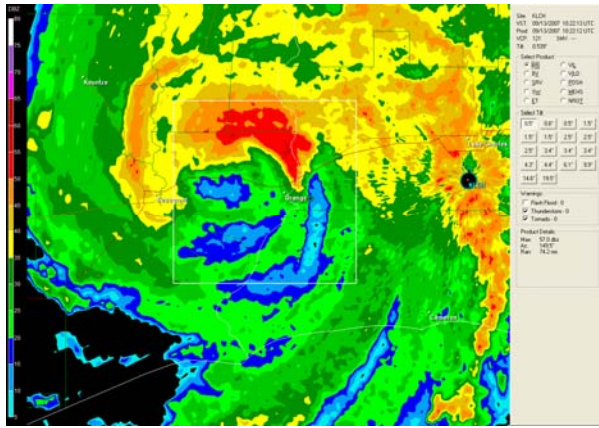
b.



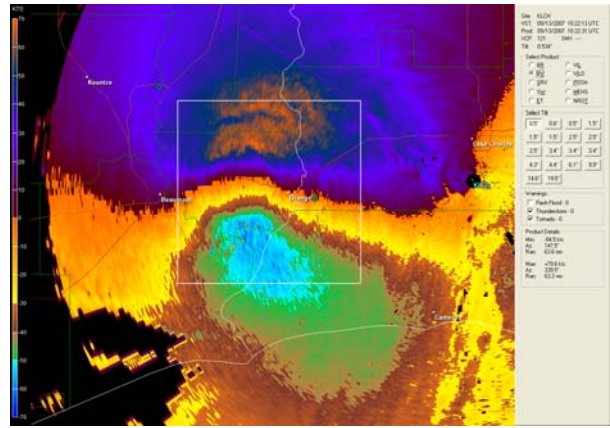
c.

Figure 10. Collapsing core in Hurricane Humberto's northern eyewall just prior to landfall on the upper Texas Coast near High Island, TX at 0550 UTC, 13 September 2007 as depicted by KHXG WSR-88D Level II data. Base

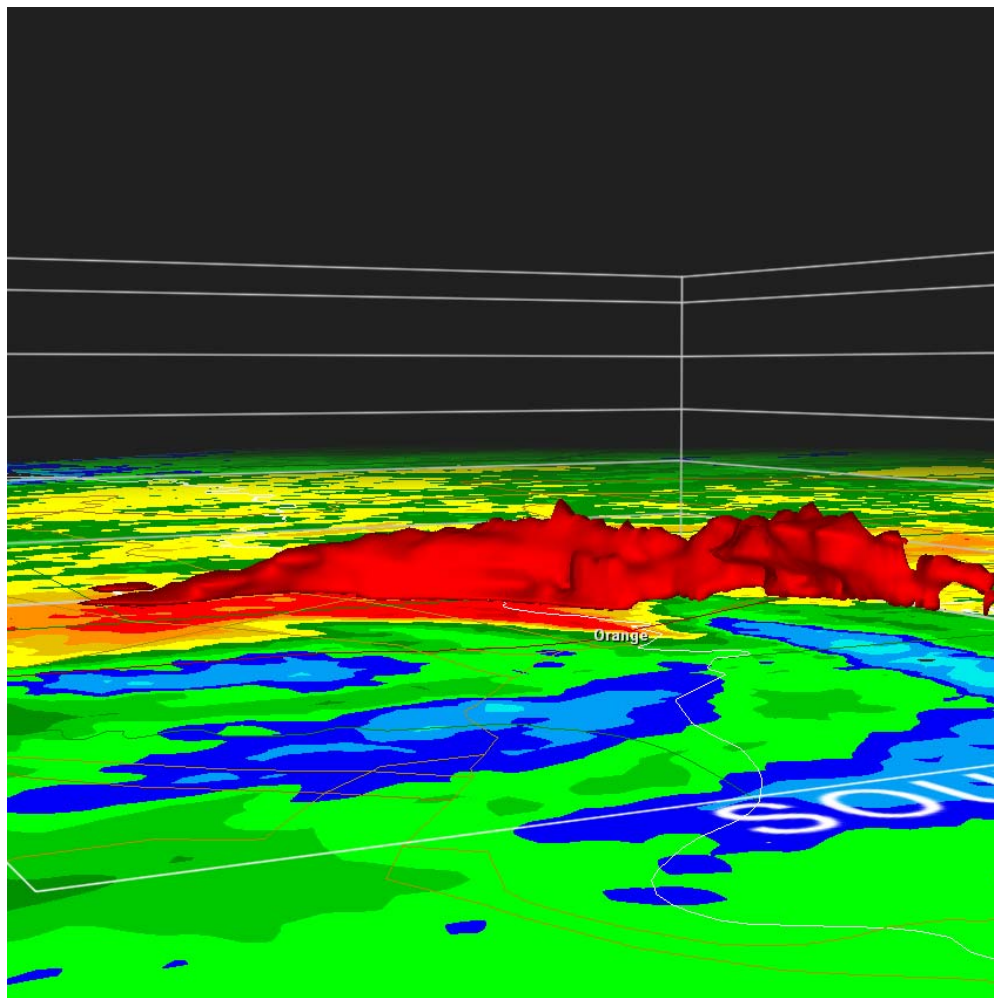
reflectivity (a.). Reflectivity cross sections through Humberto's eyewall: (b.) looking north and (c.) looking west. Red shading in a., b., and c. represents reflectivities ≥ 50 dBZ. The vertical axes in b., and c. is depicted in 10,000 foot increments [white horizontal lines].



a.



b.



c.

Figure 11. Collapsing core in Hurricane Humberto's eyewall inland in the vicinity of Orange, TX at 1012 UTC, 13 September 2007 as depicted by KLCH WSR-88D Level II data. Base reflectivity (a.). Base velocity (b.) (maximum outbound [orange]/inbound [blue] velocities: 77 kt and 64 kt, respectively). Reflectivity 3-D vertical cross sections (c.) through Humberto's eyewall looking north northeast. Red shading in a. and c. represent reflectivities ≥ 50 dBZ. The vertical axis in c., and d. is depicted in 10,000 foot increments [white horizontal lines].

Many of the very significant CCs observed in this study often contain regions of ≥ 50 dBZ reflectivity extending upward to 15,000-20,000 feet altitude, and sometimes up to near 25,000 feet in extreme cases. But there are likely numerous lower-topped CCs as well; these are more difficult to closely examine due to increasing radar beam elevation with distance.

Upon first inspection, most collapsing cores events tend to favor “open” eyewall storms, although what constitutes an “open” versus a “closed” eyewall is somewhat unclear. For instance, Hurricanes Bret, Charley (Figures 5 and 6, respectively), and Georges (near Puerto Rico and not shown) all display a “closed eyewall” in the base reflectivity pattern; however, there still remains significant variability in the reflectivity intensity pattern within these eyewalls. All three of these storms were prolific CC producers at those times. However, other storms such as Danny, Ivan, Katrina, Rita and Humberto (Figures 4, 7, 8, 9, 10, and 11, respectively) depict clearly “open eyewall” reflectivity patterns. Intrusion of dry air into the cores of these storms is likely, and may enhance the potential for negative buoyancy and even stronger downward momentum transfer/ acceleration of winds within CCs.

Precipitation patterns are highly variable between hurricanes. The CCs observed in this study displayed similar variability. The CC data collected show that CCs occur in every quadrant of the hurricane eyewall; however, it is not yet clear if one quadrant is particularly favored in the data set. For individual storms, once CC activity began in a particular quadrant, it often remained in that quadrant for periods of several hours, possibly displaying a slow temporal shift to an adjacent quadrant.

4. Future Work

More work on climatological characteristics of CC-producing storms is being performed. In addition, the HWRF numerical model will be used to provide clues to the source of some of the likely surface wind influences associated with these collapsing cores. For example, dry air intrusion into the hurricane several thousand feet above the surface will be investigated for its role in possible generation and enhancement of downbursts and extreme surface wind gusts in hurricanes. Evaporative cooling within dry air could significantly enhance the strength of

convective downburst-like features, and therefore the resulting surface winds may be stronger than with just precipitation loading only. Numerical modeling will help evaluate the potential for dry air entrainment into some of these landfalling storms and the possible enhancement of downburst-type features.

Also, areal photos and surface wind data in the vicinity of hurricane landfalls are being investigated for evidence of enhanced surface winds associated with CC activity.

5. References:

- Blackwell, K.G., 2000: The evolution of Hurricane Danny (1997) at landfall: Doppler-observed eyewall replacement, vortex contraction/intensification, and low-level wind maxima. *Monthly Weather Review* (American Meteorological Society), **128**, 4002-4016.
- Holmes, J., Blackwell, K.G., R. A. Wade, and S.K. Kimball, 2006: Collapsing precipitation cores in open-eyewall hurricanes at landfall: Are these cores actually downbursts associated with extreme surface wind gusts? *American Meteorological Society's 27th Conference on Hurricanes and Tropical Meteorology*, 24-28 April 2006, Monterey CA, Paper # 7B.7
- Medlin, J. M., S. K. Kimball, and Blackwell, K.G., 2007: Radar and Rain Gauge Analysis of the Extreme Rainfall during Hurricane Danny's (1997) Landfall, *Monthly Weather Review* (American Meteorological Society), **135**, 1869–1888.

6. Acknowledgements

Some of this work is supported by NOAA Award No. NA06NWS4680008